Spatially varying fractional flow in radial CO_2-brine displacement

Ana Mijic[1] and Tara C. LaForce[1]

Received 24 May 2011; revised 16 April 2012; accepted 13 July 2012; published 5 September 2012.

[1] In analytical modeling of two-phase flow problems in porous media, the saturation profile for a fixed time can be obtained by using the method of characteristics (MOC). One of the basic assumptions in the application of the MOC is that the fractional flow is a function of saturation only. However, when gas is injected, it is often flowing under nonlinear flow conditions and inertial losses are significant in the near-well region. Therefore, in a radial displacement non-Darcy flow applies at the injection well, but as the saturation front gets further away, its velocity will decrease and the fractional flow curve will vary with the distance along the streamline. This paper presents the extension of the Buckley-Leverett analytical solution when the injected gas phase flow is governed by the two-phase extension to the Forchheimer equation and the fractional flow function depends both on the saturation and radial distance from the well. The behavior of a gas-liquid system under non-Darcy flow conditions is shown for carbon dioxide injection into saline aquifers. Finally, this analytical solution is tested against the corresponding finite difference numerical model and the limitations of the approach are discussed.

Citation: Mijic, A., and T. C. LaForce (2012), Spatially varying fractional flow in radial CO_2-brine displacement, *Water Resour. Res.*, *48*, W09503, doi:10.1029/2011WR010961.

1. Introduction

[2] Carbon dioxide capture and storage is an important technology for reducing atmospheric emissions of carbon dioxide (CO_2) from human activities and hence mitigate climate change [*Parry et al.*, 2007]. The behavior of the injected gas can be modeled numerically, using either field-scale simulators [*Pruess*, 1987; *Schlumberger GeoQuest*, 2002] or problem specific models [*Mathias et al.*, 2009b]. However, due to the ease of implementation and computational efficiency, CO_2 injection problems are often analyzed using analytical solutions to multiphase flow, which are correct under the assumptions made for their derivation. Although a simplified approach limits their application for the analysis of specific field storage problems, analytical solutions improve the understanding of how specific aspects of the physics affect the injection process. Furthermore, they can be used as a benchmark to validate numerical solutions of a full physics world.

[3] Two-phase displacement of immiscible liquids through porous media can be analytically described with the Buckley-Leverett formulation [*Buckley and Leverett*, 1942], which assumes a one-dimensional (1-D), homogeneous reservoir and incompressible phases. The equations of momentum for the phases are modeled by Darcy's law. By introducing the concept of the fractional flow, the Buckley-Leverett solution was derived for the case of horizontal flow and negligible capillary pressure.

[1]Department of Earth Science and Engineering, Imperial College London, London, UK.

Corresponding author: A. Mijic, Department of Earth Science and Engineering, Imperial College London, South Kensington Campus, London SW7 2AZ, UK. (ana.mijic08@imperial.ac.uk)

0043-1397/12/2011WR010961

[4] The Buckley-Leverett equation is a form of a scalar hyperbolic conservation law with a nonconvex flux function [*LeVeque*, 1994]. Since the initial state can be defined with the piecewise constant data, this Riemann problem can be solved using the method of characteristics (MOC). The implementation of MOC for the analysis of multiphase flow problems is also given by *Bedrikovetsky* [1993] and *Orr* [2007]. By following the characteristics, the saturation profile can be constructed for any fixed time after the beginning of the injection process. However, the result is a multivalued solution, which is physically impossible as it indicates that two different phase saturations can exist at a same location within the reservoir. In order to find a unique solution, it is necessary that a saturation discontinuity or a shock front forms. The velocity of the shock is found by satisfying the condition of conservation of volume across the shock, i.e., by implementing the Rankine-Hugoniot relation. Furthermore, the unique solution for a nonconvex flux function has to satisfy the Oleinik entropy condition [*LeVeque*, 1994]. For the two-phase flow example it implies that the shock velocity equals to the wave velocity on the upstream side of the shock [*Orr*, 2007]. In practice, entropy conditions that characterize shock dynamics are implemented through the equal-area rule. Since the condition of material balance for the injected fluid has to be satisfied, the integral of the discontinuous weak solution must be the same as the area bounded by the uncorrected profile. This enables the determination of the shock location at any fixed time [*LeVeque*, 1994].

[5] The fractional flow method was derived for water-oil systems and therefore has a wide application for analyzing oil recovery processes [*Pope*, 1980; *Orr*, 2007]. However, if it is applied to gas-liquid systems, such as CO_2 injection into saline aquifers, the problem of flow nonlinearity arises. The gas or supercritical CO_2, being a low-viscosity fluid, has a flow velocity that is more than an order of magnitude greater than the one for a liquid phase for the same pressure change

[*Dake*, 1998]. Therefore, for many gas injection problems equations describing the flow of a gas phase through a porous formation should include the nonlinear component.

[6] The nonlinear flow conditions in water-oil systems were examined by several authors. The numerical solutions to multiphase non-Darcy displacement are presented by *Wu* [2002] and *Ahmadi et al.* [2009]. Moreover, *Wu* [2001] presents the analytical solution to the nonlinear two-phase flow problem, assuming that both phases flow under non-Darcy conditions in a 1-D system. The presented solution shows that the nonlinear displacement is controlled not only by relative permeability curves but also by the level of inertial losses and flow injection rates. More recently, the solutions for the radial and composite flow systems based on non-Darcy flow models of Forchheimer and Barree and Conway are presented by *Wu et al.* [2010]. *Wu et al.* [2011] developed the general analytical and numerical solution with the Barree and Conway model.

[7] Although presented solutions significantly contribute to understanding the nonlinear behavior of multiphase flow, they assume that the same fractional flow function applies to the whole displacement and that the nonlinear parameters dominate the displacement process even when the shock front has moved further away from the injection well. This models a 1-D core flood, but it is incorrect for radial flow in a reservoir. In radial flow, the non-Darcy component is the most significant in the area of large pressures gradients close to the well [*Dake*, 1998; *Mathias et al.*, 2009b]. As the saturation front advances into a reservoir, the influence of nonlinear parameters diminishes and the flow conditions become Darcian. Hence the fractional flow function should change with the position from the well. Furthermore, in existing solutions the non-Darcy flow conditions are assumed for both flowing phases. However, in a gas-liquid displacement, the injection phase nonlinearity is the dominant behavior, and it can be assumed that the liquid phase flows under Darcian conditions.

[8] Introduction of the fractional flow dependency on both saturation and radial distance from the well leads to the nonclassical form of a hyperbolic problem. The characteristics are not straight lines, because the wave velocity can change with the distance. The saturation, as a dependent variable, varies along a characteristic. However, due to the continuity condition for the interface between subdomains, the flux function is constant along a characteristic [*Bedrikovetsky*, 1993]. The spatially varying flux function problems can be solved either numerically [*LeVeque*, 2002] or by solving two sets of ordinary differential equations that define the characteristics and variation of the solution in time [*LeVeque*, 1994].

[9] The problem of the fractional flow function dependence on parameters other than saturation can be found in the analysis of the water drive displacement of non-Newtonian oil [*Bedrikovetsky*, 1993]. In that work it is assumed that the water phase is a Newtonian fluid and it displaces non-Newtonian oil with an arbitrary nonlinear flow behavior. The Buckley-Leverett solution can be applied, but in this case the fractional flow curve is a function of a displacement velocity. The application of this approach to improved oil recovery analysis is given by *Rossen et al.* [2008]. They extended the fractional flow theory to non-Newtonian fluids where fluid viscosity changes with a radial position and implemented it to the modeling of foam and polymer displacement processes.

[10] In this paper, the nonlinear flow behavior of a gas phase is modeled by replacing the Darcy's model with a two-phase extension of the Forchheimer equation [*Liu et al.*, 1995; *Evans and Evans*, 1988]. The liquid phase is assumed to flow under Darcian conditions. The fractional flow curve is a function of both saturation and radial distance from the well. The saturation profile is obtained by implementing the generalized MOC [*Greenberg*, 1978], where the characteristic equation is solved by numerical integration. However, in contrast to the Buckley-Leverett approach, the characteristic equation is solved with values of fluxes fixed along the curves. The location of the shock front is determined by the equal-area rule. The proposed solution is applied to the modeling of CO_2 injection into saline aquifers, with a comparison to the corresponding numerical solution. Furthermore, limitations of the proposed approach with the respect to the full physics of the problem are discussed.

2. Mathematical Model for the Nonlinear Two-Phase Displacement

[11] When the effects of dispersion are neglected and by applying the concept of a fractional flow, the radial convection equation for a gas phase in two-component, two-phase incompressible flow can be written as

$$\frac{\partial S_1}{\partial t} + \frac{Q}{\pi H \phi} \frac{\partial f_1}{\partial (r^2)} = 0 \tag{1}$$

where S is phase saturation, t [T] is time, Q [L^3 T^{-1}] is injection flow rate, H [L] is aquifer thickness, ϕ is aquifer porosity, f is phase fractional flow and r [L] is a radial distance from the well. The derivation of equation (1) assumes a constant flux along the entire saturated thickness of the aquifer. Subscripts define phases considered, such that subscript 1 represents injected gas or supercritical CO_2, while subscript 2 is used for the resident liquid. The details of the derivation of the radial convection equation are given in Appendix A. Equation (1) is analogous to the Buckley–Leverett model [*Buckley and Leverett*, 1942]

$$\frac{\partial S_1}{\partial t} + \frac{Q}{A \phi} \frac{\partial f_1}{\partial x} = 0 \tag{2}$$

with two differences: (i) equation (1) is developed for a radial flow geometry, while equation (2) assumes linear (1-D) reservoir and (ii) in equation (2) the fractional flow is a function of a saturation only, while equation (1) allows the functional dependence of the fractional flow to both saturation and a radial distance from the well. The latter difference enables the application of equation (1) in analysis of two-phase flow under spatially varying nonlinear conditions.

[12] In order to reduce the number of variables, the following dimensionless transformations in space and time, respectively can be applied [*Rossen et al.*, 2008]

$$r_D = \frac{r^2}{r_e^2} \tag{3}$$

$$t_D = \frac{Qt}{\pi r_e^2 H \phi} \tag{4}$$

where r_e [L] is radial extent of the reservoir unit. Substitution of equations (3) and (4) simplifies the governing differential equation (1) to

$$\frac{\partial S_1}{\partial t_D} + \frac{\partial f_1}{\partial r_D} = 0. \tag{5}$$

[13] In order to solve equation (5) it is necessary to define the functional dependence of the gas fractional flow, i.e., the relation $f_1 = f_1(S_1, r_D)$. In this paper it is assumed that the gas phase flows under nonlinear conditions and the two-phase extension of the Forchheimer equation [*Liu et al.*, 1995; *Evans and Evans*, 1988] is valid

$$-\frac{dP}{dr} = \frac{\mu_1}{kk_{r1}} q_1 + b_1 \rho_{v1} q_1 |q_1| \tag{6}$$

where P [M L^{-1} T^{-2}] is fluid pressure, μ [M L^{-1} T^{-1}] is dynamic viscosity, k [L^2] is intrinsic permeability, k_r is relative permeability, q [L T^{-1}] is fluid velocity, b [L^{-1}] is the Forchheimer parameter and ρ_v [M L^{-3}] is mass density. The liquid phase flows under linear conditions and the two-phase extension of the Darcy's law [*Dake*, 1998] can be applied

$$q_2 = -\frac{kk_{r2}}{\mu_2} \frac{dP}{dr} \tag{7}$$

The gas phase relative permeability can be obtained based on the model presented by *Corey* [1954]

$$k_{r1} = (1 - s)^2 \left(1 - (s)^2\right) \tag{8}$$

where

$$s = \frac{S_2 - S_{2r}}{1 - S_{2r} - S_{1c}} \tag{9}$$

and indexes r and c represent the residual saturation of the liquid phase and the critical saturation of the gas phase, respectively. Relative permeabilities for the liquid phase can be found using the parametric model for predicting the hydraulic conductivity of the two-phase flow obtained by *Luckner et al.* [1989]. The model is an extension of the approach suggested by *van Genuchten* [1980] for the estimation of the hydraulic conductivity of the single-phase flow system. If the scaled variable is defined as

$$\bar{S} = \frac{S_2 - S_{2r}}{1 - S_{2r}} \tag{10}$$

then the relative permeability of the liquid phase is

$$k_{r2} = (\bar{S})^l \left\{ \left[1 - (1 - \bar{S})^{1/m} \right]^m \right\}^2 \tag{11}$$

where l is a pore connectivity for liquid phase and m is van Genuchten model parameter.

[14] The linear behavior of the liquid phase enables direct calculation of a phase velocity q_2 and implementation into the fractional flow function. However, the governing partial differential equation for the gas flow is nonlinear and in order to determine the value of q_1 some form of linearization technique has to be applied. In this paper linearization is achieved by rearranging equation (6) such that

$$q_1 = -\frac{kk_{r1}}{\mu_1} \frac{dP}{dr} \left(1 + \frac{b_1 \rho_{v1} kk_{r1}}{\mu_1} |q_1| \right)^{-1} \tag{12}$$

The following terms are defined

$$B_1 = \frac{b_1 \rho_{v1} kk_{r1}}{\mu_1} \tag{13}$$

and

$$q_1^0 = -\frac{kk_{r1}}{\mu_1} \frac{dP}{dr} \tag{14}$$

Equation (13) defines parameter B_1. As the gas is assumed to be incompressible and the phase density does not depend on the pressure, the parameter is a function of gas saturation only ($B_1 = B_1(S_1)$). In order determine the value of parameter B_1, it is necessary to calculate the Forchheimer coefficient for the gas phase, b_1. In this paper the approach presented by *Wu* [2001] is implemented and the following model is used

$$b_1 = \frac{C_b}{(kk_{r1})^{5/4} [\phi(S_1 - S_{1c})]^{3/4}} \tag{15}$$

where C_b [L$^{3/2}$] the is non-Darcy flow constant. Furthermore, the linear fraction of gas flow velocity, q_1^0 can be defined using equation (14). Finally, equation (12) transforms into

$$q_1 = \frac{q_1^0}{1 + B_1 |q_1|} \tag{16}$$

which leads to the specification of factor F defined as

$$F = 1 + B_1 |q_1| \tag{17}$$

Factor F is treated as a coefficient and it is assumed to be a scalar function of the magnitude of local flux at any point [*Choi et al.*, 1997]. The value of the gas phase flow velocity q_1 exists on both sides of equation (16), so the problem has to be solved iteratively. Furthermore, the pressure gradient dP/dr in equation (14) is an unknown variable. However, the mass conservation equation [*Wu*, 2001]

$$Q = \sum_{j=1}^{2} q_j A = (q_1 + q_2) 2r\pi H \tag{18}$$

has to be satisfied and that condition is used for the determination of phase velocities and the pressure gradient. Starting from an initial guess for dP/dr distribution in the considered domain, the factor F is evaluated using previous (known) values of the solution. This allows for the pressure gradient to be determined under the assumptions of nonlinear flow conditions at the new iteration level. This procedure is referred to as the Picard iterative method [*Stephenson and Radmore*, 1990] and was successfully implemented by *Mijic* [2009] for the linearization of the governing continuity equation for the numerical solution of the two-dimensional nonlinear single-phase flow. Appendix B gives more details of the applied iterative procedure.

Table 1. Parameters for the Application Example for the Modeling of nonlinear Flow During CO_2 Injection Into a Saline Aquifer

Parameter	Value	Units
Permeability k	10^{-13}	m^2
Porosity ϕ	0.12	dimensionless
Aquifer thickness H	100	m
Radial extent of the reservoir r_e	1000	m
Well radius r_w	0.1	m
Initial pressure P_0	12	MPa
Aquifer temperature T	45	°C
Injection rates Q	0.01	$m^3\ s^{-1}$
	0.05	$m^3\ s^{-1}$
	0.1	$m^3\ s^{-1}$
Non-Darcy flow constants C_b	3.2×10^{-7}	$m^{3/2}$
	3.2×10^{-6}	$m^{3/2}$
Critical gas phase saturation S_{1c}	0.05	dimensionless
Residual liquid phase saturation S_{2r}	0.3	dimensionless
Pore connectivity for the liquid phase l	0.5	dimensionless
van Genuchten model parameter m	0.457	dimensionless
Gas phase viscosity μ_1	4.96×10^{-5}	Pa s
Liquid phase viscosity μ_2	8.26×10^{-4}	Pa s
Equilibrium gas phase mass density ρ_{v1}	639.7	kg m^{-3}

[15] After both phase velocities have been determined and hence the value of the factor F, the fractional flow function of the gas phase for any radial distance r can be calculated as (see Appendix A)

$$f_1 = \left(1 + \frac{k_{r2}\mu_1}{k_{r1}\mu_2}F\right)^{-1} \tag{19}$$

The advantage of this approach is that when inertial losses are insignificant, the value of B_1 tends to zero and so the factor F converges to 1. Consequently, the problem simplifies to the linear flow conditions.

3. Solution by the Method of Characteristics

[16] The Buckley-Leverett solution assumes that the fractional flow f_1 in equation (5) is a function of saturation only. However, if it depends both on S_1 and r_D then the governing differential equation (5) becomes [*Rossen et al.*, 2008]

$$\frac{\partial S_1}{\partial t_D} + \left(\frac{\partial f_1}{\partial S_1}\right)_{r_D}\frac{\partial S_1}{\partial r_D} = -\left(\frac{\partial f_1}{\partial r_D}\right)_{S_1} \tag{20}$$

and characteristics have a slope

$$\frac{dr_D}{dt_D} = \left(\frac{\partial f_1}{\partial S_1}\right)_{r_D} \tag{21}$$

Equation (20) has a unique solution as long as the characteristics do not cross on a r_D-t_D diagram. At the time when they first intersect, the MOC breaks down and a modification in a form of shock wave must be introduced. Since the fractional flow function changes with the distance from the well, the characteristics are not straight lines anymore, as is the case in linear flow (see equation (21)). It also means that velocity of characteristics changes as r_D changes. The nonzero term on right-hand side of equation (20) implies that saturation is not constant along a characteristic, but the fractional flow is [*Bedrikovetsky*, 1993]. If the functional dependence between saturation and fractional flow $f_1(S_1, r)$ is defined for any distance from the well, the condition of flux continuity along a characteristic can be used for solving equation (21). Starting from the initial condition

$$r_D(f_1(S_1), 0) = r_{Dw} \tag{22}$$

the characteristic equation (21) can be integrated with a fixed value of a flux, resulting in multivalued saturation profile for a fixed time. In order remove the multivalued parts, the discontinuity or shock has to be inserted. Its location r_D^F can be determined by integrating the saturation profile using the equal-area rule

$$r_D^F = \frac{1}{S_1^F}\int_0^{S_1^F} r_D \mathrm{d}S_1. \tag{23}$$

[17] *LeVeque* [1994] proved that the Rankine-Hugoniot condition holds even when the discontinuity propagates with a variable speed, as is the case in the two-phase nonlinear flow. The instantaneous shock velocity at time t can be calculated with values of saturation at the left and the right side of the shock evaluated at the same time.

4. Application Example

[18] The described procedure for modeling of the nonlinear two-phase flow is implemented for the analysis of the CO_2 injection test Problem 3, presented in the Lawrence Berkeley National Laboratory intercomparison project [*Pruess et al.*, 2002]. The input data are presented in Table 1. Mass density of the gas phase, ρ_{v1} for the given temperature and pressure is calculated using the fluid property estimation model presented by *Mathias et al.* [2009a]. Non-Darcy flow constant values are taken from *Wu* [2001]. Injection rate values are assumed, while all the other parameters are taken from *Pruess et al.* [2002]. In order to find the solution to the variable fractional flow function, radial axis r_D is discretized into $N = 1000$ equally spaced nodes, at which the non-Darcy gas velocity is iteratively calculated.

[19] Gas and liquid phase relative permeability curves are presented in Figure 1. They were calculated using equations (8) and (11) respectively, with the model parameters given in Table 1. Equation (15) was used to determine the dependence of the Forchheimer parameter for gas phase b_1 on the phase saturation. By analyzing equation (15) it can be concluded that as the gas phase becomes less mobile, that is, saturation approaches the value of the residual, the influence of non-Darcy effect is more significant. However, if the influence of the gas phase flow velocity is included, the composite effect of flow nonlinearity can be analyzed through the behavior of the factor F (see equation (17)). Figure 2 shows that influence of the non-Darcy effect is restricted to very narrow area around the well. At the radial distances larger than couple of meters, the values of factor F are becoming nearly constant and are approaching limit value of $F = 1$ in Darcian flow conditions. It can be also seen that the significant increase of b_1 values for low gas saturations

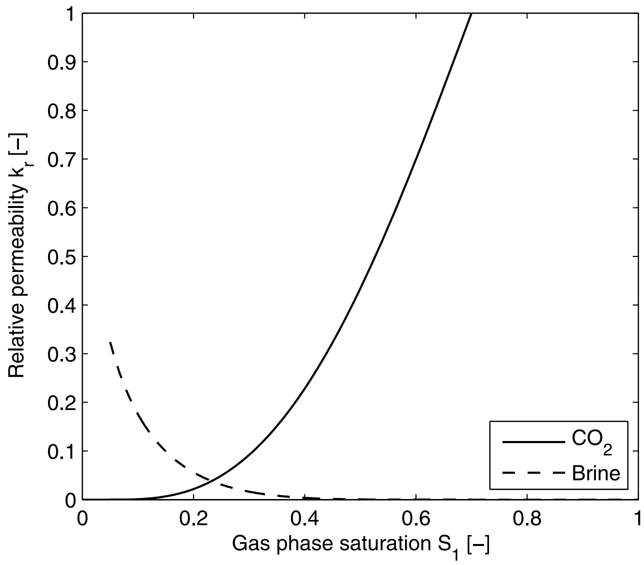

Figure 1. Relative permeability curves for gas and liquid phases.

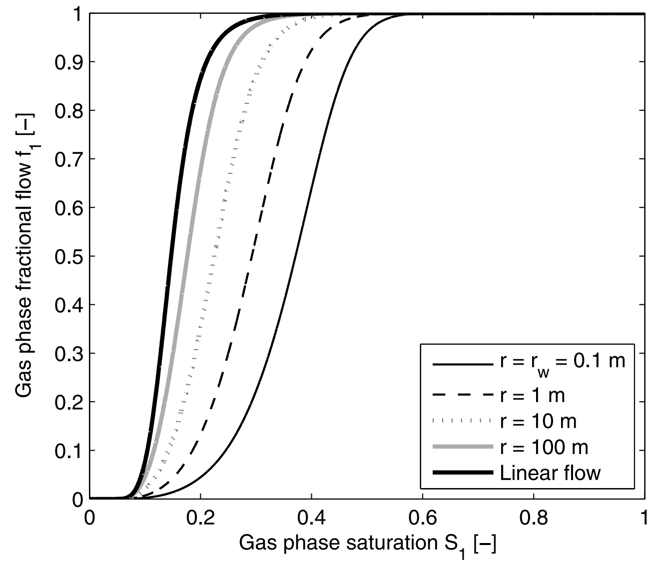

Figure 3. Fractional flow curves as a function of gas phase saturation and radial distance from the well for $Q = 0.05$ m^3 s^{-1} and $C_b = 3.2 \times 10^{-6}$ m$^{3/2}$.

does not necessary imply large pressure increase at the injection well in equation (6). However, the pressure buildup in the wellbore area will be greater than in laminar flow conditions.

[20] When the influence of the inertial losses is defined, it is possible to determine the fractional flow curve for any radial distance from the well by following the iterative procedure presented in section 2. Fractional flow curves for several distances from the well for set injection rate and non-Darcy flow constant are presented in Figure 3. It shows the expected response from the system to the nonlinear flow conditions. The most significant influence of the non-Darcy effect is near the well where, for a given saturation value, the inertial losses significantly slow down the gas phase flow. As the gas front advances inside the reservoir, the nonlinear flow fraction becomes less significant, and the flow conditions are approaching Darcian (thick black line in Figure 3). The extent of the non-Darcy effect will depend on reservoir characteristics as well as on the injection rate and assumed level of flow nonlinearity, defined through the coefficient C_b.

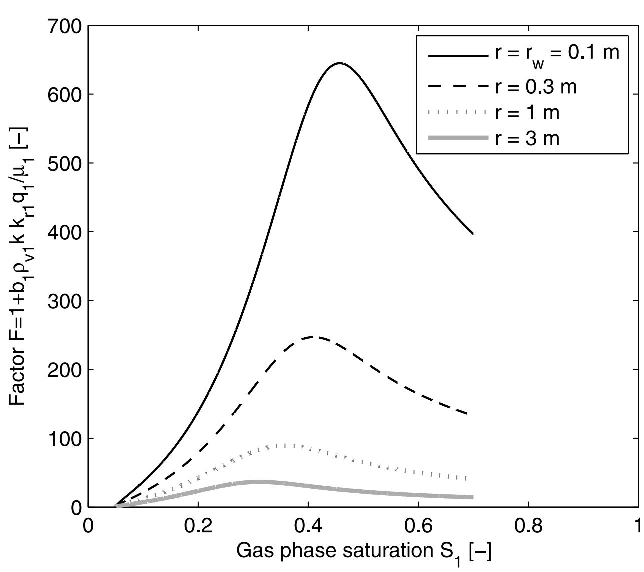

Figure 2. The flow nonlinearity as a function of gas phase saturation. Factor F is defined in equation (17) and has a constant value of $F = 1$ in linear flow conditions. The non-Darcy flow constant is $C_b = 3.2 \times 10^{-6}$ m$^{3/2}$, and the injection rate is $Q = 0.05$ m^3 s^{-1}.

[21] Since determination of the non-Darcy gas phase velocity involves Picard iterative procedure, the convergence of the scheme was tested. Table 2 presents the influence of the non-Darcy flow constant C_b and radial distance from the well r on the number of iterations required to meet the error tolerance criteria. The results show that a good initial assumption for the pressure distribution enables the iterative procedure to be computationally very efficient. For all the analyzed scenarios, the scheme converges in less than 30 iterations. On the other hand, the method is sensitive to the variation of C_b and r. As the divergence from the linear flow conditions increases, i.e., at the locations closer to the well and with higher non-Darcy flow constant, more iterations are needed in order to get the correct solution.

[22] Saturation profiles and shock fronts for any combination of parameters can be calculated using equations (21) and (23), respectively. One interesting aspect of the non-Darcy displacement is its influence on the shock front

Table 2. Performance of the Picard Scheme: Number of Iterations as a Function of Non-Darcy Flow Constant C_b and Radial Distance From the Well r

	C_b (m$^{3/2}$)		
r (m)	3.2×10^{-7}	3.2×10^{-6}	3.2×10^{-5}
0.1	21	24	27
1	20	21	24
10	16	20	21
100	8	16	20

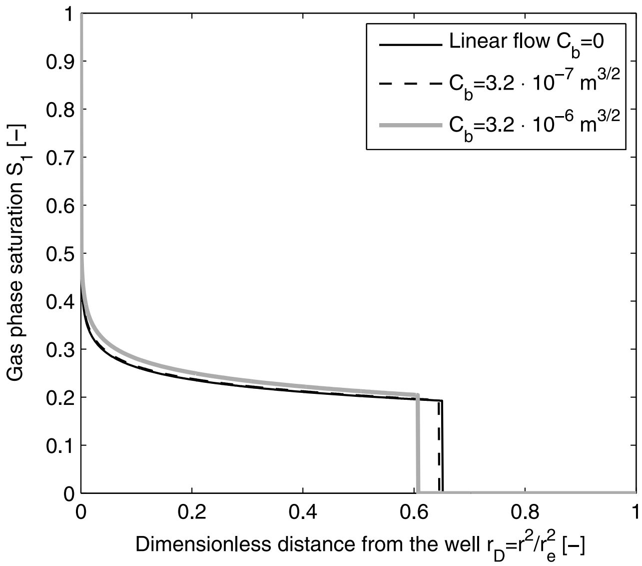

Figure 4. Saturation profiles of Darcy and nonlinear displacements. The time is in dimensionless units and equal to t_D = 0.15. The injection rate is Q = 0.05 m^3 s^{-1}.

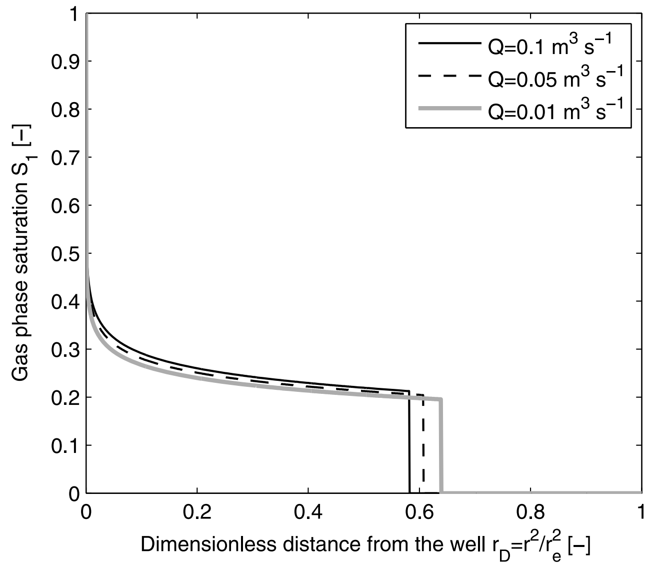

Figure 5. Saturation profiles of nonlinear displacement for constant injection volume. The time is in dimensionless units and equal to t_D = 0.15. The non-Darcy flow constant is $C_b = 3.2 \times 10^{-6}$ $m^{3/2}$.

characteristics (Figure 4). As the wave velocity is a function of both saturation and the non-Darcy flow constant, the shock front will travel much slower in the case of nonlinear flow. The explanation is the same as for the fractional flow curves: inertial losses slow down the gas phase flow as compared to the same parameters in Darcian flow conditions (C_b = 0). Consequently, more liquid phase is displaced from the reservoir. This is favorable for CO_2 injection processes as the higher gas saturations imply larger storage capacity. Neglecting the nonlinear behavior can also lead to the overestimation of the lateral extent of the gas plume.

[23] Although in linear flow conditions the saturation profiles are not dependent on the injection rate, when non-Darcy displacement is assumed this is not the case. The influence of the variable injection rate can be analyzed by fixing the injection volume, i.e., by setting the fixed dimensionless time t_D. Figure 5 shows that the shock front moves more slowly for the faster, more turbulent injection, which is due to the larger flow resistance to the gas phase when injection rate is increased. Therefore, higher injection rates will enhance the nonlinear effect, which will result in higher gas saturations and hence better displacement efficiency. If the maximal allowable injection pressure is not reached, increased injection rate allows for larger volumes of CO_2 to be stored in a given reservoir volume.

[24] The influence of the flow nonlinearity on the characteristic velocity is presented in Figure 6. Shock saturations (dots in Figure 6) obtained from equation (23) follow the corresponding characteristic velocity curve, which shows that both Rankine-Hugoniot and entropy conditions are satisfied. Like the fractional flow function, the characteristic velocity is changing with the distance from the well. Furthermore, as the shock front advances, the shock front saturation decreases. However, the influence of the non-Darcy effect diminishes as the front moves further into the reservoir. Eventually, the solution will approach the linear flow conditions, after which the shock front will continue to advance with constant velocity and saturation.

[25] Finally, the non-Darcy effect on the pressure buildup is analyzed. Once the saturation profile is determined, pressure gradient dP/dr_D can be calculated for every radial distance from the well. Equation (B6) from Appendix B can then be numerically integrated with respect to r_D to obtain the value of pressure buildup dP. Results are presented in Figure 7, with x axis set logarithmically to emphasize the near-well area. The rapid pressure increase close to the well is expected, due to the significant influence of inertial losses in

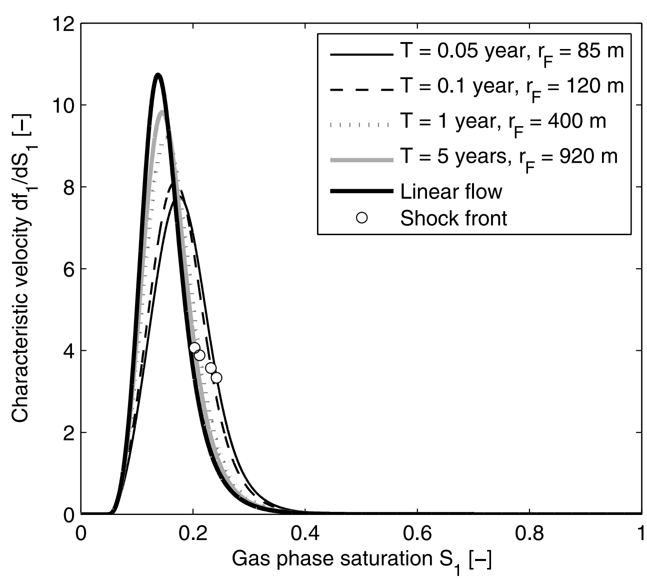

Figure 6. Characteristic velocity profiles for a shock front at different time levels. The non-Darcy flow constant is C_b = 3.2×10^{-6} $m^{3/2}$, and the injection rate is Q = 0.05 m^3 s^{-1}.

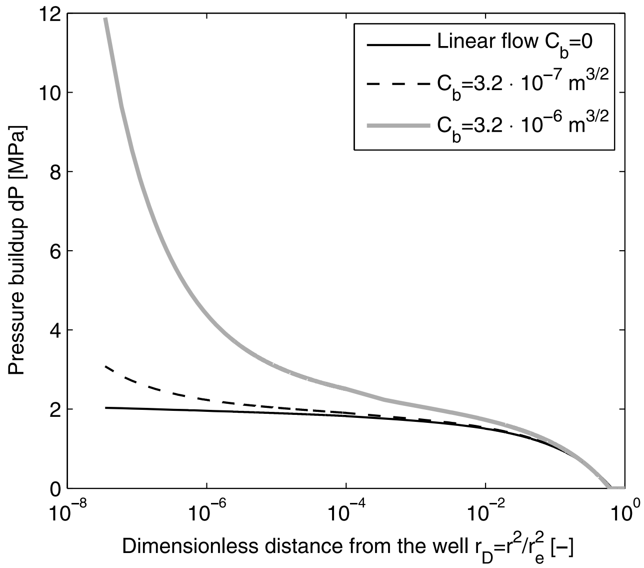

Figure 7. Pressure buildup during the injection process for Darcy and nonlinear flow conditions. The time is in dimensionless units and equal to t_D = 0.15. The injection rate is Q = 0.05 m^3 s^{-1}.

that zone. It can also be seen that as the flow nonlinearity increases, the non-Darcy influence disseminates further inside the reservoir. Another interesting feature of the pressure plot is a large increase of dP near the well as C_b changes for an order of magnitude from 10^{-7} to 10^{-6}. This could indicate the threshold value of the non-Darcy flow for a given aquifer when the pressure buildup could induce the fracturing of the reservoir rock.

5. Comparison With a Finite Difference Solution

[26] In order to validate the presented approach, equation (5) was solved numerically using forward finite difference with an implicit scheme. For every time level, the following numerical representation of the problem

$$\frac{\Delta S_1}{\Delta t_D} = -\frac{\left(f_{1\,i+1} - f_{1\,i}\right)}{\Delta r_D} \tag{24}$$

is solved in MATLAB with ordinary differential equation solver ode15s. The indices i and i + 1 represent current and forward space nodes in radial direction, respectively. The values of $f_1 = f_1(S_1, r_D)$ are calculated by implementing the same iterative scheme as used in the analytical solution.

[27] Simulation results are presented in Figure 8. The numerical grid has intervals equal to Δr_D = 0.001. The same resolution is used in the analytical simulation used for comparison. The plot shows excellent agreement between the numerical and analytical solutions, verifying the proposed approach to the nonlinear modeling of the two-phase flow systems.

6. Limitations of the Proposed Solution

[28] The application of the proposed solution for the analysis of full physics problems is limited by the underlying assumptions of phases' immiscibility and incompressibility. In Darcian flow conditions, effects of CO_2 compressibility on storage in saline aquifers were analyzed by *Vilarrasa et al.* [2010]. They concluded that the influence on the interface position is not significant when viscous forces dominate. However, the pressure estimation was overestimated when gas compressibility was neglected. *Mathias et al.* [2011] examined the role of partial miscibility on pressure buildup. The well pressure declined due to the development of the dry-out zone and a corresponding increase in CO_2 relative permeability in the near-well region. Also, the leading front saturation in a case of miscible displacement will be higher than when the phase behavior is neglected. Therefore, when Darcian flow conditions are valid, both phase behavior and compressibility will contribute to the lowering of reservoir pressures and increasing the leading shock front saturation.

[29] In non-Darcy flow conditions, it can be assumed that the effects of compressibility and miscibility will become even more significant. Under the assumption of gas incompressibility, the parameter B_1 (see equation (13)), which defines the level of flow nonlinearity, is a function of saturation only. In pressure-dependent flow conditions, however, its value will additionally vary due to the influence of the gas mass density. As the nonlinear effects are the most significant in the vicinity of the well, it is expected that gas compressibility will have a positive effect on injectivity and reduce the pressure peak that occurs at the well. Miscible non-Darcy flow is expected to reduce evaporation in a near-well region and therefore contribute to the reduction of solid salt precipitation. Furthermore, combined with the compositional displacement, reduction in pressure due to CO_2 compressibility will additionally affect evaporation of water and dissolution of CO_2 in aqueous phase. Hence, the nonlinear solution proposed in this work is likely to overestimate well pressure and underestimate saturation distribution,

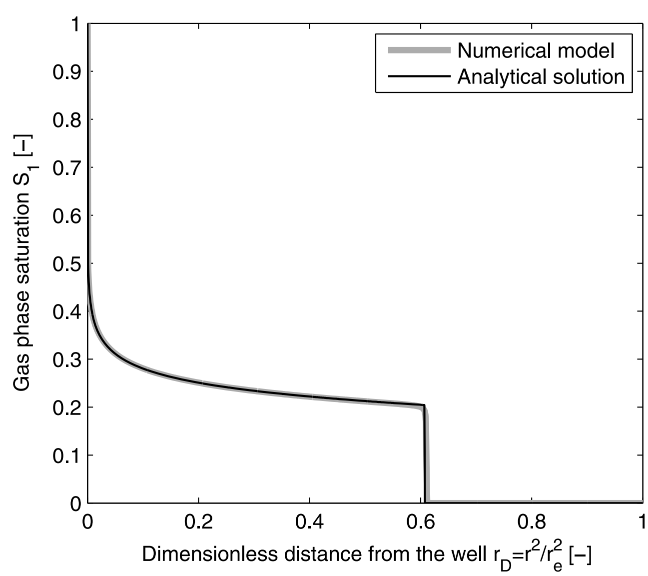

Figure 8. Comparison between analytical and numerical solution. The time is in dimensionless units and equal to t_D = 0.15. The non-Darcy flow constant is C_b = 3.2 × 10^{-6} $m^{3/2}$, and the injection rate is Q = 0.05 m^3 s^{-1}.

which gives the worst-case scenario solution for a given set of input data.

7. Summary

[30] Analytical solutions to two-phase flow systems are a useful tool for preliminary analysis of complex problems such as CO_2 injection into saline aquifers. Though the well-established Buckley-Leverett formulation is successfully implemented in variety of oil recovery analysis, the gas-liquid problems require the extension of the model in order to account for the nonlinear behavior of the gas phase in the near-well region.

[31] This paper presents the development of the analytical model for radial, nonlinear two-phase flow, in which fractional flow is a function of both saturation and the distance from the well. Using the presented iterative procedure, equation (19) can be used for the calculation of non-Darcy fractional flow function. Furthermore, the solution for the saturation profiles and shock front can be obtained by using equations (21) and (23), respectively.

[32] It was shown that the inertial losses are the most significant in an area close to the well (Figure 3). As the distance from the well increases, the flow conditions become Darcian, and the classical Buckley-Leverett solution can applied. Figures 4 and 5 show that in nonlinear systems, the phase saturation is controlled not only by the relative permeability functions, but also by the injection rate and the magnitude of the inertial losses, defined by the constant C_b. In addition, the shock front velocity and saturation are changing in time (Figure 6). As the shock front moves further from the well, its saturation decreases but the shock advances faster until the Darcian limit is reached. The analysis of the pressure buildup (Figure 7) showed that there is a limiting value of non-Darcy constant bellow which pressure increases negligibly comparing to Darcian conditions. Once that value is reached, there is a significant additional pressure buildup that could limit the rate of gas injection. The validity of the proposed solution was confirmed by the comparison with the corresponding numerical model and presented in Figure 8. Finally, it was argued that by neglecting the effects of compressibility and miscibility, the proposed solution gives the limiting values of both well pressure and shock saturation.

8. Conclusions

[33] The preliminary analysis of CO_2 sequestration scenarios requires a reliable tool which enables taking into account as many characteristics of two-phase systems behavior as possible. The selection of the injection rate for CO_2 sequestration is a trade-off between the larger storage capacity over a short period of time and the larger pressure buildup. It was shown that if the non-Darcy displacement is assumed to be valid, the conditions for CO_2 storage are even more favorable than in the linear flow conditions due to better displacement efficiency. The gas front will advance slower and will occupy more volume within the same period of time. However, this comes at the cost of higher injection pressure at the well.

[34] Additional work has to be undertaken in order to examine the level of gas flow nonlinearity likely to occur in reservoirs suitable for CO_2 injection at reasonable injection rates, to confirm the values of non-Darcy flow constants used in the presented model. Furthermore, the extension of the solution with the compressible and miscible modules and its comparison to commercial simulators would significantly contribute to its applicability for a real storage analysis.

Appendix A: The Conservation Equation for Radial Two-Phase Flow

[35] The conservation of the mass of a gas phase has to satisfy the following:

$$\underbrace{\left[(r+\Delta r)^2 - r^2\right]\pi H \phi \Delta(S_1\rho_1)}_{\text{Change in storage}} = \underbrace{2r\pi H \Delta t \rho_1 q_1}_{\text{Mass in}} - \underbrace{2(r+\Delta r)\pi H \Delta t[\rho_1 q_1 + \Delta(\rho_1 q_1)]}_{\text{Mass out}} \tag{A1}$$

Rearranging equation (A1) and assuming infinitesimal Δr and Δt leads to

$$\phi \frac{\partial(S_1\rho_1)}{\partial t} = -\frac{\rho_1 q_1}{r} - \frac{\partial(\rho_1 q_1)}{\partial r} \tag{A2}$$

Furthermore, if fluid is assumed to be incompressible (ρ_1 = const.), then the conservation equation for a gas phase is

$$\frac{\partial S_1}{\partial t} + \frac{1}{\phi}\left[\frac{q_1}{r} + \frac{\partial q_1}{\partial r}\right] = 0 \tag{A3}$$

The same conservation equation can be written for a liquid phase

$$\frac{\partial S_2}{\partial t} + \frac{1}{\phi}\left[\frac{q_2}{r} + \frac{\partial q_2}{\partial r}\right] = 0 \tag{A4}$$

Adding equations (A3) and (A4) yields

$$\frac{\partial(S_1+S_2)}{\partial t} + \frac{1}{\phi}\left[\frac{1}{r}(q_1+q_2) + \frac{\partial(q_1+q_2)}{\partial r}\right] = 0 \tag{A5}$$

The sum of phase saturations has to be 1.0 and therefore is constant. Consequently, the time derivative in equation (A5) is equal to zero. In addition, the total flow velocity is defined as a sum of phase velocities, $q_1 = q_1 + q_2$. Therefore, the change of the total flow velocity in radial direction is

$$\frac{\partial q}{\partial r} = -\frac{q}{r} \tag{A6}$$

Using the concept of a fractional flow, where $f_1 = q_1/q$, equation (A3) can be written as

$$\frac{\partial S_1}{\partial t} + \frac{1}{\phi}\left[\frac{f_1 q}{r} + \frac{\partial}{\partial r}(f_1 q)\right] = 0 \tag{A7}$$

Substituting equation (A6) into equation (A7) and applying the product rule for the derivative of a product of functions $f_1 = f_1(r)$ and $q = q(r)$ yields

$$\frac{\partial S_1}{\partial t} + \frac{q}{\phi}\frac{\partial f_1}{\partial r} = 0 \tag{A8}$$

Total flow velocity in equation (A8) can be expressed as a function of volumetric injection flow rate Q or as a linear flow rate as $q = Q/A$, where the cross-sectional area is

$A = 2r\pi H$. Finally, the radial conservation equation for a gas phase is obtained as

$$\frac{\partial S_1}{\partial t} + \frac{Q}{\pi H \phi}\frac{\partial f_1}{\partial (r^2)} = 0. \quad \text{(A9)}$$

[36] In equation (A9) the fractional flow function is defined as

$$f_1 = \frac{q_1}{q} = \frac{q_1}{q_1 + q_2} \quad \text{(A10)}$$

Substitution of equations (7) and (16) into equation (A10) yields

$$f_1 = \frac{\frac{q_1^0}{F}}{\frac{q_1^0}{F} + q_2} = \frac{-\frac{kk_{r1}}{\mu_1}\frac{dP}{dr}\frac{1}{F}}{-\frac{kk_{r1}}{\mu_1}\frac{dP}{dr}\frac{1}{F} - \frac{kk_{r2}}{\mu_2}\frac{dP}{dr}} \quad \text{(A11)}$$

where F is defined as in equation (17). Rearrangement of equation (A11) gives the final form of the nonlinear fractional flow model

$$f_1 = \frac{1}{1 + \frac{k_{r2}\mu_1}{k_{r1}\mu_2}F}. \quad \text{(A12)}$$

Appendix B: Iterative Calculation of the Gas Phase Velocity

[37] In order to be consistent with the dimensionless form of the conservation equation (5), the flow governing equations have to be transformed as well. The relation given in equation (3) is used, which transforms equations (16), (7) and (18), respectively into

$$q_1 = -\frac{kk_{r1}}{\mu_1}\frac{2\sqrt{r_D}}{r_e}\frac{dP}{dr_D}(1 + B_1 q_1)^{-1} = q_1^0(1 + B_1 q_1)^{-1} \quad \text{(B1)}$$

$$q_2 = -\frac{kk_{r2}}{\mu_2}\frac{2\sqrt{r_D}}{r_e}\frac{dP}{dr_D} \quad \text{(B2)}$$

$$Q = (q_1 + q_2)2r_e\sqrt{r_D}\pi H \quad \text{(B3)}$$

For the calculation of the gas phase velocity q_1 the following algorithm is suggested:

[38] 1. An initial pressure gradient $(dP/dr_D)^i$ is determined assuming linear flow conditions for both flowing phases ($B_1 = 0$). Substitution of equations (B1) and (B2) into (B3) gives

$$\left(\frac{dP}{dr_D}\right)^i = -\frac{Q}{4r_D\pi Hk}\left(\frac{k_{r1}}{\mu_1} + \frac{k_{r2}}{\mu_2}\right)^{-1}. \quad \text{(B4)}$$

[39] 2. Values of $(dP/dr_D)^i$ are then used for the calculation of Darcian fraction of gas phase velocity $q_1 = q_1^0$ using equation (B1) with $B_1 = 0$.

[40] 3. In order to account for the flow nonlinearity, equation (B1) is rearranged into the form of a quadratic equation $B_1 q_1^2 + q_1 - q_1^0 = 0$, whose solution is the gas phase velocity in non-Darcy conditions

$$q_1 = \frac{-1 + \sqrt{1 + 4B_1 q_1^0}}{2B_1}. \quad \text{(B5)}$$

[41] 4. Based on the value of q_1 from the previous step, the value of factor F is calculated using equation (17).

[42] 5. The new value of the pressure gradient dP/dr_D is then calculated under the assumption of nonlinear flow conditions for the gas phase as

$$\frac{dP}{dr_D} = -\frac{Q}{4r_D\pi Hk}\left(\frac{1}{F}\frac{k_{r1}}{\mu_1} + \frac{k_{r2}}{\mu_2}\right)^{-1}. \quad \text{(B6)}$$

[43] 6. Values of $(dP/dr_D)^i$ and dP/dr_D are then compared. If the difference is larger than the defined tolerance error, the procedure is repeated with the updated values of pressure gradients until the convergence criteria is satisfied.

[44] **Acknowledgment.** The authors would like to acknowledge the support of the Grantham Institute for Climate Change, an Institute of Imperial College London.

References

Ahmadi, A., A. A. Arani, and D. Lasseux (2009), Numerical simulation of two-phase inertial flow in heterogeneous porous media, *Transp. Porous Media*, *84*, 177–200, doi:10.1007/s11242-009-9491-1.

Bedrikovetsky, P. (1993), *Mathematical Theory of Oil and Gas Recovery*, 2nd ed., 575 pp., Kluwer Academic, Dordrecht, Netherlands.

Buckley, S. E., and M. C. Leverett (1942), Mechanism of fluid displacement in sands, *Trans. AIME*, *146*, 107–116.

Choi, E. S., T. Cheema, and M. R. Islam (1997), A new dual-porosity/dual-permeability model with non-Darcian flow through fractures, *J. Pet. Sci. Eng.*, *17*(3–4), 331–344.

Corey, A. T. (1954), The interrelation between gas and oil relative permeabilities, *Prod. Mon.*, *19*, 38–41.

Dake, L. P. (1998), *Fundamentals of Reservoir Engineering*, 17th ed., 498 pp., Elsevier Sci., Amsterdam, Netherlands.

Evans, E. V., and R. D. Evans (1988), Influence of an immobile or mobile saturation on non-Darcy compressible flow of real gases in propped fractures, *J. Petrol. Technol*, *40*(10), 1343–1351.

Greenberg, M. D. (1978), *Foundations of Applied Mathematics*, Prentice-Hall, Englewood Cliffs, N. J.

LeVeque, R. J. (1994), *Numerical Methods for Conservation Laws*, Birkhäuser Verlag, Basel, Switzerland.

LeVeque, R. J. (2002), *Finite Volume Methods for Hyperbolic Problems*, Cambridge Univ. Press, Cambridge, U. K.

Liu, X., F. Civan, and R. D. Evans (1995), Correlation of the non-Darcy flow coefficient, *J. Can. Pet. Technol.*, *34*(10), 50–54.

Luckner, L., M. T. Van Genuchten, and D. R. Nielsen (1989), A consistent set of parametric models for the two-phase flow of immiscible fluids in the subsurface, *Water Resour. Res.*, *25*(10), 2187–2193.

Mathias, S., P. Hardisty, M. Trudell, and R. Zimmerman (2009a), Screening and selection of sites for CO_2 sequestration based on pressure buildup, *Int. J. Greenhouse Gas Control*, *3*, 577–585, doi:10.1016/j.ijggc.2009.05.002.

Mathias, S. A., P. E. Hardisty, M. R. Trudell, and R. W. Zimmerman (2009b), Approximate solutions for pressure buildup during CO_2 injection in brine aquifers, *Transp. Porous Media*, *79*(2), 265–284, doi:10.1007/s11242-008-9316-7.

Mathias, S. A., J. G. Gluyas, G. J. González Martínez de Miguel, and S. A. Hosseini (2011), Role of partial miscibility on pressure buildup due to constant rate injection of CO2 into closed and open brine aquifers, *Water Resour. Res.*, *47*, W12525, doi:10.1029/2011WR011051.

Mijic, A. (2009), Forchheimer flow in multiple well systems, MSc thesis, Imp. Coll. London, London.

Orr, F. M. (2007), *Theory of Gas Injection Processes*, Tie-Line Publ., Holte, Denmark.

Parry, M. L., O. F. Canziani, J. P. Palutikof, P. J. Van der Linden, and C. E. Hanson (Eds.) (2007), *IPCC Climate Change 2007: Impacts, Adaptation and Vulnerability. Contribution of Working Group II to the Fourth Assessment Report of the Intergovernmental Panel on Climate Change*, Cambridge Univ. Press, Cambridge, U. K.

Pope, G. (1980), The application of fractional flow theory to enhanced oil recovery, *Old SPE J.*, *20*(3), 191–205.

Pruess, K. (1987), TOUGH user's guide, Div. of Waste Manage., Off. of Nucl. Mater. Safety and Safeguards, U.S. Nucl. Regul. Comm., Washington, D. C.

Pruess, K., J. Garcia, T. Kovscek, C. Oldenburg, J. Rutqvist, C. Steefel, and T. Xu (2002), Intercomparison of numerical simulation codes for geologic disposal of CO_2, *Tech. Rep. LBNL-51813*, Lawrence Berkeley Natl. Lab., Berkeley, Calif.

Rossen, W. R., R. T. Johns, K. R. Kibodeaux, H. Lai, and N. M. Tehrani (2008), Fractional-flow theory applied to non-Newtonian IOR processes, paper presented at 11th European Conference on the Mathematics of Oil Recovery, ECMOR Sci. Comm., Bergen, Norway, 8–11 Sept.

Schlumberger GeoQuest (2002), Eclipse 300 technical description, Houston, Tex.

Stephenson, G., and P. M. Radmore (1990), *Advanced Mathematical Methods for Engineering and Science Students*, Cambridge Univ. Press, Cambridge, U. K.

van Genuchten, M. T. (1980), A closed-form equation for predicting the hydraulic conductivity of unsaturated soils, *Soil Sci. Soc. Am. J.*, *44*(5), 892–898.

Vilarrasa, V., D. Bolster, M. Dentz, S. Olivella, and J. Carrera (2010), Effects of CO_2 compressibility on CO_2 storage in deep saline aquifers, *Transp. Porous Media*, *85*(2), 619–639, doi:10.1007/s11242-010-9582-z.

Wu, Y. S. (2001), Non-Darcy displacement of immiscible fluids in porous media, *Water Resour. Res.*, *37*(12), 2943–2950.

Wu, Y. S. (2002), Numerical simulation of single-phase and multiphase non-Darcy flow in porous and fractured reservoirs, *Transp. Porous Media*, *49*(2), 209–240.

Wu, Y. S., P. Fakcharoenphol, and R. Zhang (2010), Non-Darcy displacement in linear composite and radial flow porous media, paper presented at SPE EUROPEC/EAGE Annual Conference and Exhibition, Soc. of Pet. Eng., Barcelona, Spain.

Wu, Y. S., B. Lai, J. L. Miskimins, P. Fakcharoenphol, and Yuan D. (2011), Analysis of multiphase non-Darcy flow in porous media, *Transp. Porous Media*, *88*, 205–223, doi:10.1007/s11242-011-9735-8.